Analytical Methods

Accepted Manuscript

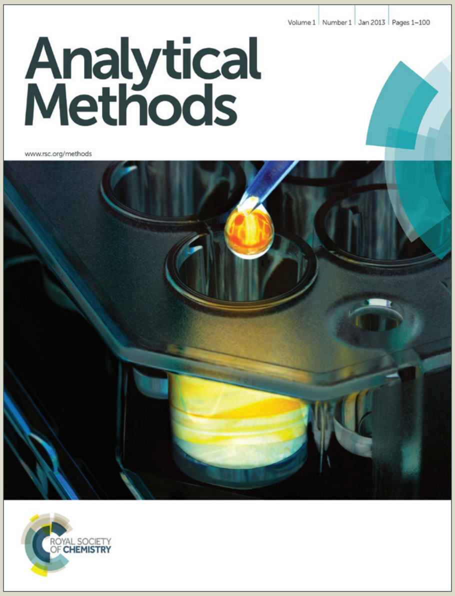

ROYAL SOCIETY
OF **CHEMISTRY**

www.rsc.org/methods

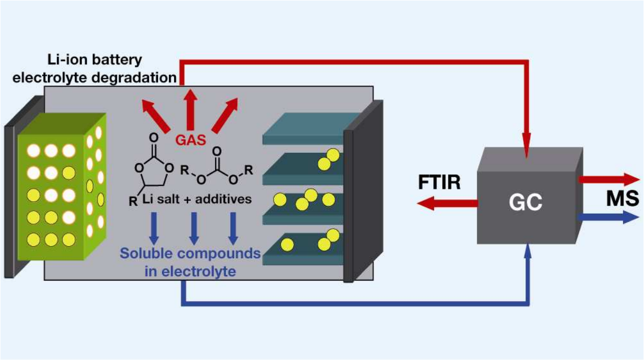

Li-ion battery organic electrolyte is the critical compound responsible for capacity decay and thermal runaway phenomenon. A coupling tool for volatile and soluble electrolytes degradation compounds analysis is proposed.

Table of contents

Gas Chromatography/Fourier Transform Infrared/Mass Spectrometry Coupling: a Tool for Li-Ion Battery Safety Field Investigation

Grégory Gachot[a,b], Sylvie Grugeon[a,b], Isabel Jimenez-Gordon[a,b,c], Gebrekidan Gebresilassie Eshetu[a,b,d], Simeon Boyanov[d], Amandine Lecocq[d], Guy Marlair[d], Serge Pilard[e], Stephane Laruelle[*a,b]

[a] Laboratoire de Réactivité et de Chimie des Solides, UMR CNRS 7314, Université de Picardie Jules Verne, 33 rue Saint Leu, 80039 Amiens, France

[b] Réseau sur le Stockage Electrochimique de l'Energie (RS2E), FR CNRS 3459, France

[c] DGMPE, Renault, 1 avenue du Golf, 78288 Guyancourt, France

[d] Institut National de l'Environnement Industriel et des Risques (INERIS), Parc Technologique Alata, BP2, 60550 Verneuil-en-Halatte, France

[e] Plate-Forme Analytique, Université de Picardie Jules Verne, 33 rue Saint Leu, 80039 Amiens, France

Corresponding author : stephane.laruelle@u-picardie.fr

Tel : +33 322827585 Fax : +33 322827585

Keywords: Li-ion battery, ageing, safety, Gas Chromatography/Mass Spectrometry, Gas Chromatography/Fourier Transform Infrared/Mass Spectrometry

ABSTRACT

As electric vehicles may have a positive impact on global warming, worldwide endeavour is devoted to improving the performance, durability and safety of the Li-ion batteries considered as the most promising technology. To help the characterisation and identification of volatile compounds released upon batteries ageing or during a system malfunction-induced thermal event, we implemented the coupling of the gas chromatography (GC) technique with mass spectrometry (MS) and Fourier transform infrared (FTIR) analytical tools. Through two detailed examples related to the thermal runaway phenomenon and the battery swelling, this paper provides evidences that the complementarities of these techniques allow us to detect and then accurately identify a vast array of volatile molecules ensuing from electrochemically/chemically driven electrolyte degradation. Hence, this GC/FTIR/MS equipment will be powerful in studying the impact of new electrolytes molecules on the battery functioning or safety and in assessing its degradation state after long-term or unexpected premature capacity loss.

1 INTRODUCTION

In the environmental context of global warming, the high energy density makes the Li-ion batteries the most attractive technology and thus an obvious choice for up-and-coming plug-in and pure electric vehicles powering. However, this implies that the batteries must meet durability and safety requirements[1–5], often still perceived as actual challenges for high power or high energy applications. For this purpose, for a few years many researchers have been developing a vast array of techniques to diagnose concerns downstream. For instance, non-destructive electrochemical impedance spectroscopy and modelling are under investigation, giving the opportunity to follow/predict interfaces resistive and capacitive contributions upon ageing[6–8]. Moisture-free environment performing state-of-the-art techniques enable interfacial compounds chemical nature (XPS [9]...) identification and content assessment that help go back to the origin of failure mechanisms. The issues consumers could be faced with are i) the Li-ion batteries capacity loss while being maintained under pretty harsh conditions such as scorching heat or ii) battery swelling due to dendrite-induced short-circuit or overcharge in case of a failure in the battery management system. In both cases, the electrolyte is thermally and/or electrochemically decomposed and these reactions entail the release of gases and volatile soluble compounds.

Within the framework of the RS2E (French research network on electrochemical energy storage) network thematic devoted to Battery Safety, we are developing experimental protocols to study these events[10–14]. In order to identify the extensive range of volatile compounds with the highest possible index of recognition, we came up with the idea of coupling gas chromatography (GC) techniques with mass spectrometry (MS) and Fourier transform infra-red (FTIR) analytical tools. This coupled technique was originally developed in the 80's by Wilkins[15–17] and permits complementary analysis by IR and MS in the fragrance and essential oils fields[18].

Through two detailed examples relevant to the Li-ion batteries safety field, this paper points out to the genuine reasons that make such coupled techniques efficient and deserving more use for safety or environment-focused applications in relation with energy storage. The first example deals with the thermal runaway phenomenon and more specifically with the characterization of volatile compounds released upon heating of a lithiated negative electrode active material in contact with electrolyte[12]. The second example concerns the analysis of the gaseous species and the most volatile soluble molecules recovered from a swollen commercial battery.

2 EXPERIMENTAL SECTION

2.1 GC conditions

Gas: All analyses were performed using a trace GC ultra gas chromatograph (Thermo Scientific). The analysed gases were transferred into the split/splitless injector maintained at 200°C. The chromatographic separation was performed on a “HP-PLOT/Q” polystyrene-divinylbenzene-based capillary column (30 m × 0.32 mm i.d., 20 µm) from Agilent J & W Technologies followed by a post capillary column “Rtx-1” (15 m × 0.25 mm i.d., 0.25 µm, 100% dimethyl polysiloxane) from Restek.

Liquid: The analyses were performed using a trace 1300 series GC ultra gas chromatograph (Thermo Scientific). The chromatographic separation was performed on a “BPX70” cyanopropyl polysilene-siloxane based capillary column (30 m × 0.25 mm i.d., 0.25 µm) from SGE.

2.2 FTIR conditions

The GC was interfaced with a light-pipe GC/FTIR system (Thermo Scientific) and connected to a FTIR system Nicolet 6700 with a mid-infrared source and a medium band, liquid nitrogen cooled mercury cadmium telluride (MCT) detector. Aldrich vapour phase FTIR library was used to identify the infrared spectra.

2.3 MS conditions

The GC was interfaced with an ISQ mass spectrometer (Thermo Scientific). Compounds identification and corresponding structural formulae were assigned using the National Institutes of Standards (NIST) library.

More details on the coupled technique are placed in the subsection A of the Supplementary Information section.

2.4 Indexation criteria

The large number of peaks of the reported Gram-Schmidt and chromatograms resulting from the GC/FTIR/MS analyses were assigned with the help of confidence indexes given by the software after matching with libraries. Identification of the molecules was considered to be correct after the following criteria were fulfilled. For a given peak, if the confidence index is higher than 70% in both techniques or higher than 90% in only one of the techniques, IR spectrum and fragmentation pattern are compared with those of the libraries. Only this ultimate visual test validates the identification result.

3 RESULTS AND DISCUSSION

3.1 General findings and reminders about concerned coupling techniques

The gas chromatography coupled with analyzers is being developed to investigate Li-ion battery organic electrolytes ageing and thermal reactions[4,10,19–25]. The gas chromatography / mass spectrometry is the mainly used technique[12,13]. However, this has some intrinsic limitations; i) according to the molecules volatility, change of chromatographic column is required to analyze the overall degradation compounds[12,13,26], ii) the single data base from which the compounds are recognized is not exhaustive and, finally, iii) the peaks intensity on the chromatogram not only depends on the compounds concentration but also on their ionization capability; a compound which hardly ionizes is more difficult to detect. The IR detector is less sensitive than the MS one; however it allows the identification of components by providing functional groups and using different data bases. Moreover, the Gram-Schmidt peaks intensity is linked to the IR spectra peaks area and not to their ionization capability. An ultimate advantage of the IR technique is that it enables detection of volatile compounds that could be masked under MS peak of inert gas (N_2, Ar) used for moisture-sensitive molecules handling. Each of these analytical tools brings features that are complementary enough to consider coupling them through a GC/FTIR/MS system, with the aim of gaining insight into reaction mechanisms involved in battery failure events.

3.2 Instrumentation lay-out and procedure development

Figure 1 shows a diagram of the GC/FTIR/MS system configuration that has been ultimately optimized to prevent air contamination and to avoid temperature change-related gas condensation. Note that attempting to connect IR and MS detectors in series in a previous configuration failed to provide valuable data owing to chromatographic peaks broadening and air-tightness in the exit connection of light-pipe concerns. After injection and separation in the GC separation column, the sample is split with a union tee; 80 % of the flow is directed to IR and 20 % to the MS. In this case, the mass spectrometer signal is not saturated while still having a good sensitivity in IR. After the union tee, the split samples are kept to high temperature with two heated transfer lines.

Furthermore, the GC/MS part is equipped with a second capillary column to make liquid injection. This enables us to characterize the volatile soluble degradation compounds stemming from electrolyte sample thus complementing the analysis obtained with the "gas" column.

Following this optimization step, we undertook the first validation tests by analyzing gases formed at 200°C at the interface between lithiated graphite negative electrode and carbonates-based electrolyte. The electrochemical cell assembling and lithiation procedures and the sample preparation for GC/FTIR/MS analysis are described in the Supporting Information section (subsections B and C).

3.3 Detection of gas species from lithiated graphite sample heated in presence of electrolyte

Li-ion batteries thermal runaway phenomenon starts at the negative electrode/electrolyte interface at around 100°C[27]. The passivation layer (Solid Electrolyte Interphase – SEI) decomposes[12], giving direct electrolyte/LiC_6 contact. The involved redox processes result in heat and gas releases that may induce over-pressurization then rupture of the battery casing. We propose to report on the characterization of these gases by means of this coupled technique to show the input of the IR spectroscopy to the MS.

Figure 2 shows the Gram-Schmidt and chromatogram from the GC/FTIR/MS analysis of the gases evolved from the lithiated graphite in contact with the ethylene carbonate (EC)/dimethyl carbonate (DMC) (1/1 w/w)-$LiPF_6$ 1M electrolyte heated sample. The reported molecules are colored according to the analyzers that permit to identify them from the indexation criteria described in the experimental section. Some gases are clearly identified by both MS and FTIR (black-colored), but many others are only identified by one of them. Interestingly, in the chromatogram, ethylene oxide and acetaldehyde that are of same chemical formula cannot be distinguished between 25.5 and 26.8 min because of their fragment peak overlapping; as shown in figures 3a and 3b, these molecules lose a CH_3 radical to give COH^+ fragment alike. Despite of these issues, as their IR spectra are totally different (Fig. 3c and 3d), they can be unambiguously identified on Gram-Schmidt. Note that the IR spectrum of ethylene oxide evidences a peak assigned to methanol around 1000 cm^{-1} of weak intensity.

The first two peaks observed in the Gram-Schmidt correspond to carbon monoxide and methane (blue-colored); these peaks, in the chromatogram, are masked by argon, the inert gas of the glove box in which the electrochemical cells are assembled. Although these are already well known as being Li-ion battery electrolyte solvents decomposition products, their presence or not, helps discriminate the electrochemical processes involved and hence identify the side precipitated or soluble products; the impact of these products over safety and ageing of the batteries are under careful investigation[28]. This figure also shows that only IR permits acetylene identification although this molecule is recognized by MS when sufficiently concentrated[13]. IR technique may also support MS results as exemplified with these molecules; ethyl formate and methyl acetate are identified by MS (red-colored) with low confidence indexes (55 and 75% respectively) while clearly recognized by FTIR (90 and 93% respectively).

On the other hand, the MS technique, owing to its higher sensitivity, allowed many molecules from peaks of weak intensity (green-colored) to be clearly identified. It has to be noticed that, surprisingly, the MeF experimental IR spectra displays a good signal/noise ratio but is not recognized by the software; this concern will be discussed in the following example.

By only MS or FTIR analyses, one would unambiguously identify 2/3 of the molecules, which emphasizes the interest of coupling these two techniques to increase the identification capability.

3.4 Detection of gaseous and volatile soluble species recovered from a swollen commercial battery

3.4.1 Detection of gaseous species

To proceed further with the validation test, we chose a typical case where only one analysis is possible, which requires high confidence degree in molecules identification. This test consisted in analyzing the gaseous species recovered from a swollen commercial Li-ion battery (Fig. 4a inset), the components and failure conditions of which were not known. In an argon-filled glove box, 0.7 mL of gas was carefully taken with a gas syringe equipped with a valve then analyzed by GC/FTIR/MS. The corresponding Gram-Schmidt and chromatogram are shown in figure 4. The main peaks of the Gram-Schmidt (Fig. 4a) have been assigned to well-known solvents degradation products (CO, CO_2, CH_4 and C_3H_8) and diethyl carbonate (DEC); the latter being a linear alkyl carbonate commonly used as electrolyte co-solvent[29] to lower the viscosity. Worth noting is that CH_4 could not originate from DEC electrochemical degradation processes but from DMC or ethyl methyl carbonate (EMC)[12]. As these co-solvents are not detected, this volatile is likely to ensue from the presence of additives. Some peaks at 20.5, 21.8, 25.8 and 32.4 min are too weak to be analyzed. Conversely, the highly intense peak at 7.8 min, characterized thanks to MS as being ethane (16.0 min), is not recognized though its spectrum is present in the IR database. This problem, also mentioned for MeF in figure 2, is likely to be due to a matching problem from the software which can be solved after introducing the experimental spectra in the database. Other gaseous species (EtF, C_4H_8...) were identified from peaks of weak intensity detected on chromatogram (Fig. 4b).

3.4.2 Detection of the volatile soluble species

Pursuing our study towards identifying all the molecules ensuing from electrolyte degradation, we undertook the cell opening and prepared the liquid electrolyte sample according to a specific experimental procedure described in the Supporting Information section (subsection D), in order to analyze the soluble compounds by means of the "liquid" GC/MS (Fig. 4c). First of all, we can recognize, besides DEC, two electrolyte co-solvents cyclic carbonates namely propylene carbonate (PC) and EC; both cyclic carbonates feature high dielectric constant, ensuring the Li salt dissociation. Others compounds are detected as 1,1-dimethylpropyl-benzene, a compound which is likely to be used as additive for overcharge protection[30]. The two following molecules, diethyl 2,5-dioxohexane dicarboxylate and diethyl oxydiethane-2,1-diyl biscarbonate are well known to originate from successive reduction then nucleophilic reactions on solvents[13,14]. Triethyl phosphate is likely to stem from solvent and $LiPF_6$ salt degradation reaction.

It is interesting to note that DEC is the highest retention time gaseous product to be detected by means of the MS and FTIR detectors while, in solution, in these chromatographic conditions, this compound exhibits the lowest retention time. This demonstrates the benefit of the liquid analysis in enlarging the detected molecules mass range.

4 CONCLUSION

The Li-ion batteries organic electrolyte is arguably the most critical compound responsible for its capacity decay upon high temperature cycling and the thermal runaway phenomenon. Hence, great efforts are made in the search for improved electrolyte components (additives, salts and solvents) and to determine their actual impact on these failure processes. Through two examples, this paper provides evidences of the usefulness of the GC/FTIR/MS analytical tool in this field when the coupling is correctly implemented and operated. From the gaseous species analyses, MS detector revealed lots of molecules owing to its higher sensitivity while FTIR detector allowed us to complete this analysis (1/3 of molecules in the first example) even recognizing highly toxic compound as ethylene oxide whose MS fragmentation pattern overlaps with that of acetaldehyde. Additionally, the injection of liquid electrolyte in the GC/MS part gives us the opportunity to detect less volatile molecules. Hence, these “gas” and “liquid” analyses are quite complementary to identify the vast array of gaseous and soluble molecules evolving from the electrolyte thermal, chemical and/or electrochemical reactivity.

ACKNOWLEDGMENTS: This work was supported by “Région de Picardie” and FEDER through the DEGAS project. The authors are grateful to David Mathiron for his technical assistance.

BIBLIOGRAPHY

1. S. C. Levy, *J. Power Sources*, 1997, **68**, 75 – 77.
2. P. Ribière, S. Grugeon, M. Morcrette, S. Boyanov, S. Laruelle, and G. Marlair, *Energy Env. Sci*, 2012, **5**, 5271–5280.
3. D. Lisbona and T. Snee, *Process Saf. Environ. Prot.*, 2011, **89**, 434 – 442.
4. G. G. Eshetu, S. Grugeon, G. Gachot, D. Mathiron, M. Armand, and S. Laruelle, *Electrochimica Acta*, 2013, **102**, 133 – 141.
5. G. G. Eshetu, S. Grugeon, S. Laruelle, S. Boyanov, A. Lecocq, J.-P. Bertrand, and G. Marlair, *Phys Chem Chem Phys*, 2013, **15**, 9145–9155.
6. I. Jiménez-Gordon, S. Grugeon, A. Débart, G. Pascaly, and S. Laruelle, *Solid State Ion.*, 2013, **237**, 50 – 55.
7. M. Kassem, J. Bernard, R. Revel, S. Pélissier, F. Duclaud, and C. Delacourt, *J. Power Sources*, 2012, **208**, 296 – 305.
8. D. Abraham, J. Knuth, D. Dees, I. Bloom, and J. Christophersen, *J. Power Sources*, 2007, **170**, 465 – 475.
9. R. Dedryvère, S. Laruelle, S. Grugeon, L. Gireaud, J. M. Tarascon, and D. Gonbeau, *J. Electrochem. Soc.*, 2005, **152**, A689–A696.
10. L. Gireaud, S. Grugeon, S. Pilard, P. Guenot, J. M. Tarascon, and S. Laruelle, *Anal. Chem.*, 2006, **78**, 3688–3698.
11. L. Gireaud, S. Grugeon, S. Laruelle, S. Pilard, and J. M. Tarascon, *J. Electrochem. Soc.*, 2005, **152**, A850–A857.
12. G. Gachot, S. Grugeon, G. G. Eshetu, D. Mathiron, P. Ribière, M. Armand, and S. Laruelle, *Electrochimica Acta*, 2012, **83**, 402 – 409.
13. G. Gachot, P. Ribière, D. Mathiron, S. Grugeon, M. Armand, J. B. Leriche, S. Pilard, and S. Laruelle, *Anal. Chem.*, 2011, **83**, 478–485.
14. G. Gachot, S. Grugeon, M. Armand, S. Pilard, P. Guenot, J. M. Tarascon, and S. Laruelle, *J. Power Sources*, 2008, **178**, 409 – 421.
15. C. L. Wilkins, G. N. Giss, G. M. Brissey, and S. Steiner, *Anal. Chem.*, 1981, **53**, 113–117.
16. T. A. Sasaki and C. L. Wilkins, *J. Chromatogr. A*, 1999, **842**, 341–349.
17. C. L. Wilkins, *Anal. Chem.*, 1994, **66**, 295A–301A.

18. B. Oberhofer, A. Nikiforov, G. Buchbauer, L. Jirovetz, and C. Bicchi, *Flavour Fragr. J.*, 1999, **14**, 293–299.
19. K. Kumai, H. Miyashiro, Y. Kobayashi, K. Takei, and R. Ishikawa, *J. Power Sources*, 1999, **81-82**, 715 – 719.
20. S. Sloop, J. Pugh, S. Wang, J. Kerr, and K. Kinoshita, *Electrochem. Solid State Lett.*, 2001, **4**, A42–A44.
21. S. E. Sloop, J. B. Kerr, and K. Kinoshita, *J. Power Sources*, 2003, **119-121**, 330 – 337.
22. C. Campion, W. Li, and B. Lucht, *J. Electrochem. Soc.*, 2005, **152**, A2327–A2334.
23. R. Mogi, M. Inaba, Y. Iriyama, T. Abe, and Z. Ogumi, *Langmuir*, 2003, **19**, 814–821.
24. L. Terborg, S. Weber, S. Passerini, M. Winter, U. Karst, and S. Nowak, *J. Power Sources*, 2014, **245**, 836 – 840.
25. Z. Ogumi, A. Sano, M. Inaba, and T. Abe, *J. Power Sources*, 2001, **97-98**, 156 – 158.
26. T. Sasaki, T. Abe, Y. Iriyama, M. Inaba, and Z. Ogumi, *J. Power Sources*, 2005, **150**, 208–215.
27. R. Spotnitz and J. Franklin, *J. Power Sources*, 2003, **113**, 81–100.
28. A. W. Golubkov, D. Fuchs, J. Wagner, H. Wiltsche, C. Stangl, G. Fauler, G. Voitic, A. Thaler, and V. Hacker, *RSC Adv.*, 2013, **4**, 3633–3642.
29. V. Etacheri, R. Marom, R. Elazari, G. Salitra, and D. Aurbach, *Energy Env. Sci*, 2011, **4**, 3243–3262.
30. M. Xu, L. Xing, W. Li, X. Zuo, D. Shu, and G. Li, *J. Power Sources*, 2008, **184**, 427 – 431.

FIGURE CAPTION

Fig. 1: Schematic diagram of the parallel GC/FTIR/MS system for the gas injection and the GC/MS system for the liquid injection.

Fig. 2: a) GC/FTIR Gram-Schmidt and b) GC/MS chromatogram of lithiated graphite (LiC_6) + EC/DMC (1/1 w/w) – $LiPF_6$ 1M electrolyte, heated at 200°C for 3h. The retention time shift of around 7 min is due to the different gases transfer line lengths to the IR and MS analyzers. The molecules are colored according to the analyzers that enable their identification; both MS and FTIR (black), only FTIR (blue) or MS (green) and only MS but with a low confidence index (red).

Fig. 3: a) Mass spectra of a) ethylene oxide and b) acetaldehyde, IR spectra of c) ethylene oxide (with trace of methanol) and d) acetaldehyde.

Fig. 4: a) GC/FTIR Gram-Schmidt, inset: picture of the swollen battery b) GC/MS chromatogram of gas formed in a swollen commercial battery c) GC/MS chromatogram of electrolyte solvent and less volatile degradation compounds formed in the battery.

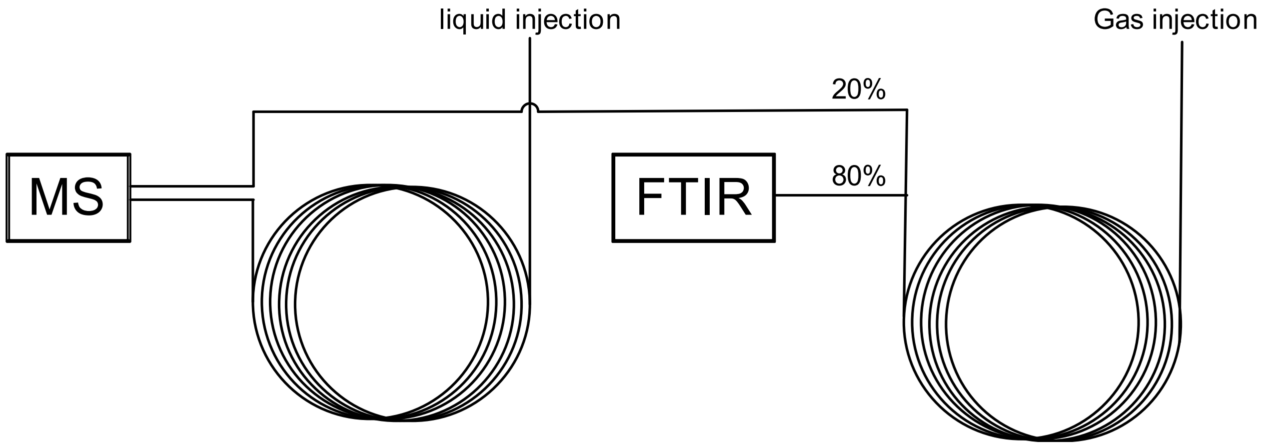

Figure 1

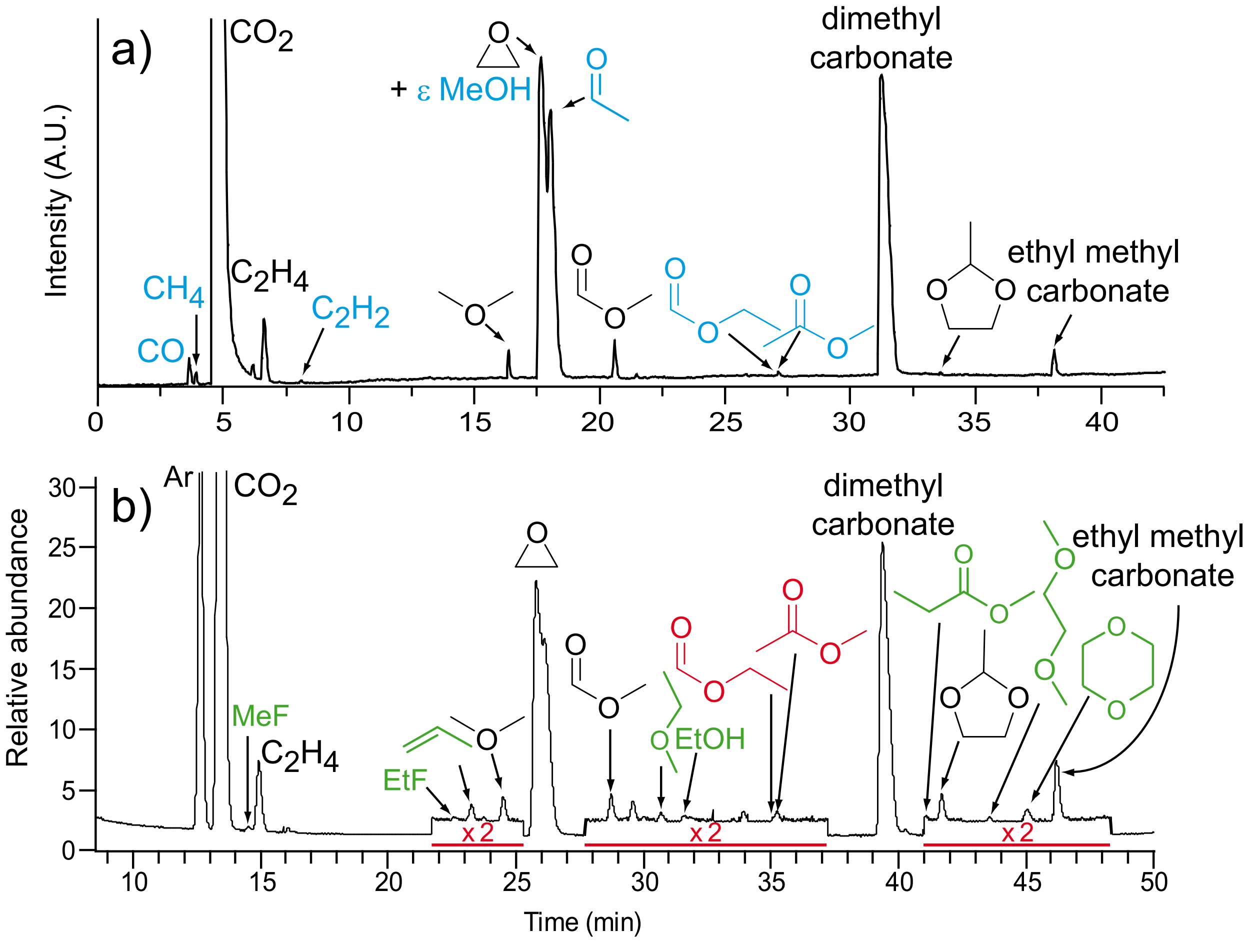
a)
Intensity (A.U.)
CO
CH_4
CO_2
C_2H_4
C_2H_2
O
+ ε MeOH
O
dimethyl carbonate
O
O
O
O
O
O
O
ethyl methyl carbonate
0
5
10
15
20
25
30
35
40
b)
Relative abundance
0
5
10
15
20
25
30
Ar
CO_2
MeF
C_2H_4
EtF
O
O
O
O
O
EtOH
O
O
O
O
dimethyl carbonate
O
O
O
O
O
O
O
O
ethyl methyl carbonate
x 2
x 2
x 2
10
15
20
25
30
35
40
45
50
Time (min)

Figure 2

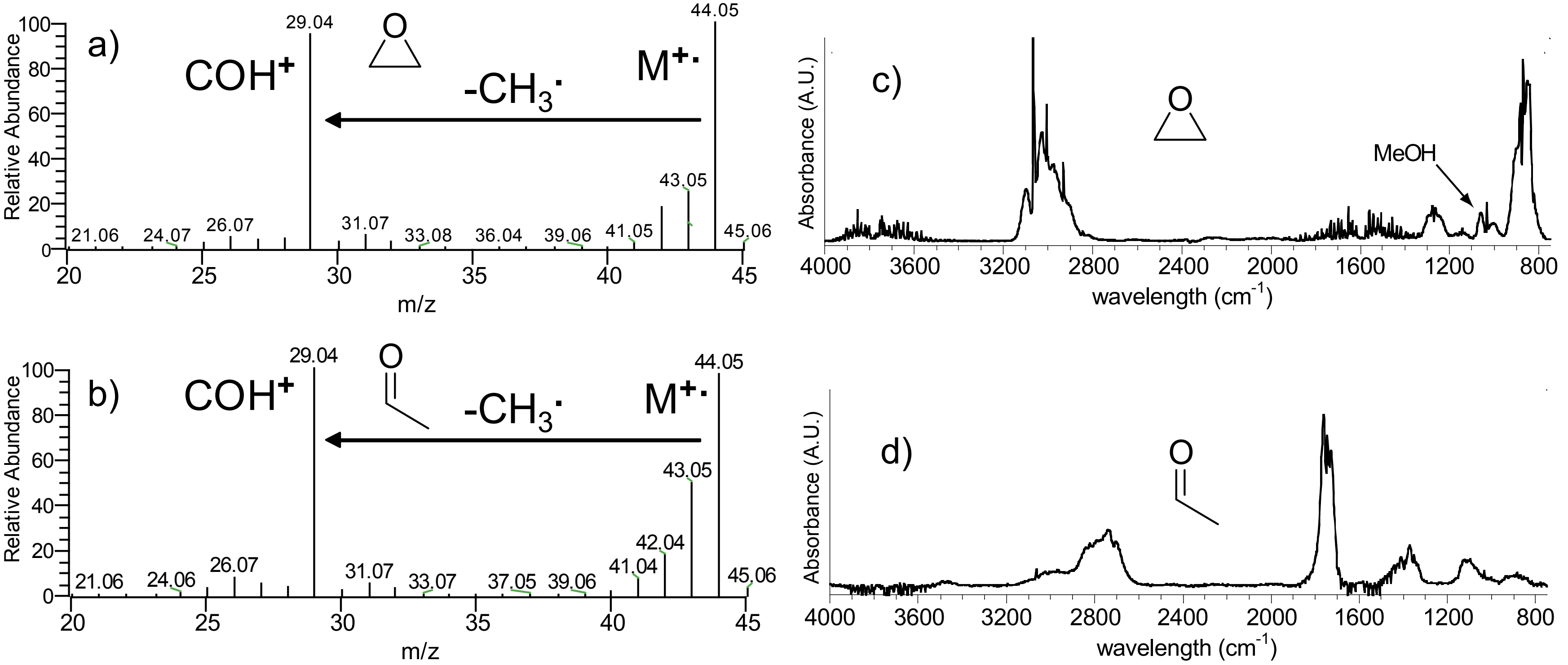
a)
Relative Abundance
100
80
60
40
20
0
COH⁺
-CH₃·
M⁺·
29.04
44.05
43.05
21.06
24.07
26.07
31.07
33.08
36.04
39.06
41.05
45.06
20
25
30
35
40
45
m/z
b)
COH⁺
-CH₃·
M⁺·
29.04
44.05
43.05
42.04
41.04
21.06
24.06
26.07
31.07
33.07
37.05
39.06
45.06
m/z
c)
Absorbance (A.U.)
MeOH
4000
3600
3200
2800
2400
2000
1600
1200
800
wavelength (cm⁻¹)
d)
Absorbance (A.U.)
wavelength (cm⁻¹)
O
O

Figure 3

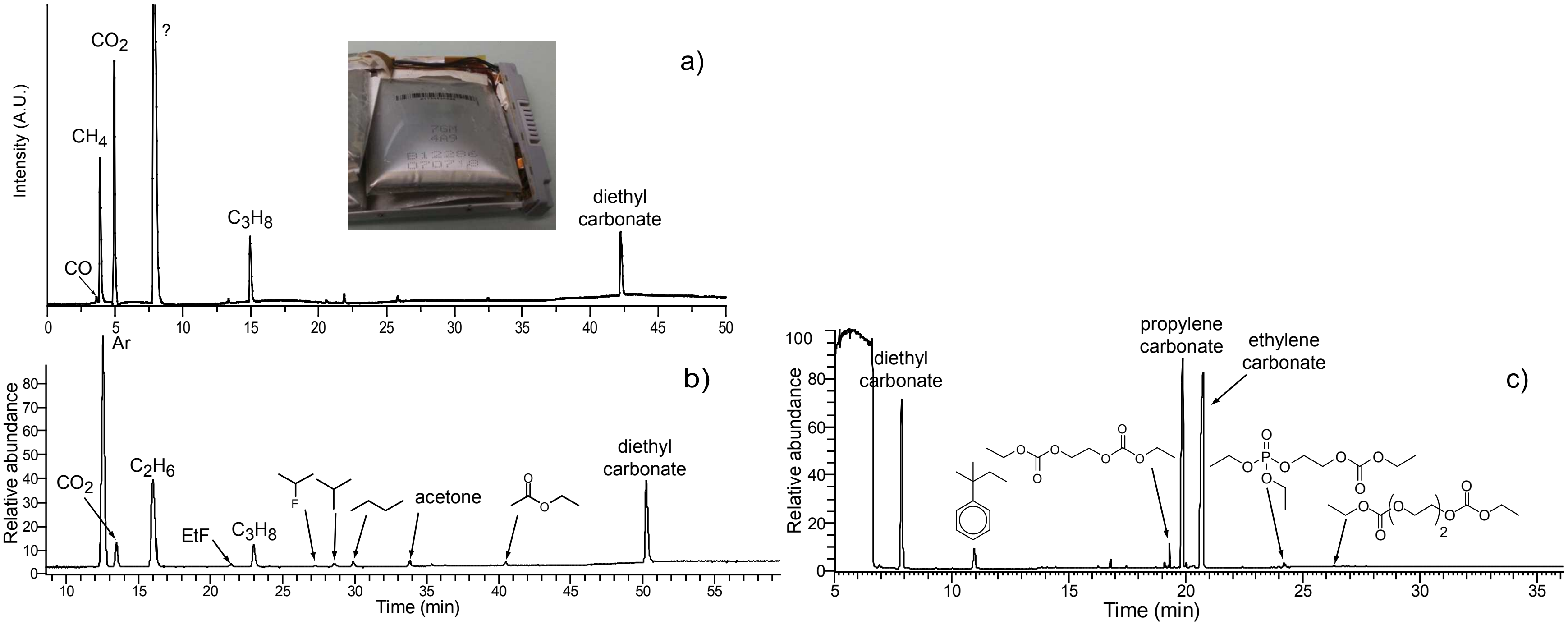
a)
Intensity (A.U.)
CO
CH4
CO2
?
C3H8
diethyl carbonate
0 5 10 15 20 25 30 35 40 45 50
Ar
b)
Relative abundance
CO2
C2H6
EtF
C3H8
F
acetone
diethyl carbonate
Time (min)
c)
Relative abundance
diethyl carbonate
propylene carbonate
ethylene carbonate
Time (min)

Figure 4